

# Magnetic interactions in NiO at ultrahigh pressure

V. Potapkin,<sup>1,\*</sup> L. Dubrovinsky,<sup>2</sup> I. Sergueev,<sup>3</sup> M. Ekholm,<sup>4</sup> I. Kantor,<sup>5</sup> D. Bessas,<sup>5</sup> E. Bykova,<sup>2</sup> V. Prakapenka,<sup>6</sup>  
R. P. Hermann,<sup>1,7</sup> R. Rüffer,<sup>5</sup> V. Cerantola,<sup>2</sup> H. J. M. Jönsson,<sup>8</sup> W. Olovsson,<sup>8</sup> S. Mankovsky,<sup>9</sup>  
H. Ebert,<sup>9</sup> and I. A. Abrikosov<sup>4,10,11</sup>

<sup>1</sup>Jülich Centre for Neutron Science (JCNS) and Peter Grünberg Institut (PGI), JARA-FIT,  
Forschungszentrum Jülich GmbH, D-52425 Jülich, Germany

<sup>2</sup>Bayerisches Geoinstitut, Universität Bayreuth, D-95440 Bayreuth, Germany

<sup>3</sup>Deutsches Elektronen-Synchrotron, D-22607 Hamburg, Germany

<sup>4</sup>Swedish e-Science Research Centre (SeRC), Department of Physics, Chemistry and Biology (IFM),  
Linköping University, SE-58183 Linköping, Sweden

<sup>5</sup>European Synchrotron Radiation Facility, Boîte Postale 220, F-38043 Grenoble, France

<sup>6</sup>CARS, University of Chicago, Chicago, Illinois 60437, USA

<sup>7</sup>Materials Science and Technology Division, Oak Ridge National Laboratory, Oak Ridge, Tennessee 37831, USA

<sup>8</sup>Department of Physics, Chemistry and Biology (IFM), Linköping University, SE-58183 Linköping, Sweden

<sup>9</sup>Department of Chemistry, Ludwig-Maximilians-University Munich, Butenandtstrasse 5-13, D-81377 Munich, Germany

<sup>10</sup>Materials Modeling and Development Laboratory, National University of Science and Technology 'MISIS', 119049 Moscow, Russia

<sup>11</sup>LACOMAS Laboratory, Tomsk State University, 634050 Tomsk, Russia

(Received 17 October 2015; revised manuscript received 26 April 2016; published 24 May 2016)

Magnetic properties of NiO have been studied in the multimegabar pressure range by nuclear forward scattering of synchrotron radiation using the 67.4 keV Mössbauer transition of <sup>61</sup>Ni. The observed magnetic hyperfine splitting confirms the antiferromagnetic state of NiO up to 280 GPa, the highest pressure where magnetism has been observed so far, in any material. Remarkably, the hyperfine field increases from 8.47 T at ambient pressure to ~24 T at the highest pressure, ruling out the possibility of a magnetic collapse. A joint x-ray diffraction and extended x-ray-absorption fine structure investigation reveals that NiO remains in a distorted sodium chloride structure in the entire studied pressure range. *Ab initio* calculations support the experimental observations, and further indicate a complete absence of Mott transition in NiO up to at least 280 GPa.

DOI: [10.1103/PhysRevB.93.201110](https://doi.org/10.1103/PhysRevB.93.201110)

Many novel materials at the frontier of solid state physics, such as high- $T_c$  superconductors, Mott insulators, spintronic materials, ferroelectrics, heavy fermion materials, etc., are examples of strongly correlated systems. In such materials, correlations between the more localized  $3d$  or  $4f$  electrons play a key role in determining the system properties.

NiO is considered one of the most important compounds for the field of strongly correlated materials for two reasons. First, it was treated as a prototype by Mott [1] to explain the nature of the insulating state that came to bear his name. Secondly, it is chemically a compound with a rather simple crystal structure, making it well suited to experimental tests of theoretical models. Before moving to more complex cases, simple cases need to be understood first. Several questions regarding the nature of the insulating state are still under discussion, e.g., the roles of the  $d-d$  and  $p-d$  splittings in forming a wide insulating band gap [2,3] of 4 eV [4].

Due to the strong Coulomb repulsion, which dominates the kinetic energy, the  $3d$ ,  $t_{2g}$ , and  $e_g$  states are widely split. Like FeO and CoO, NiO is an antiferromagnetic insulator, with a spontaneous ordering of the magnetic moments at ambient conditions, and a Néel temperature of 525 K.

It has been predicted that under sufficiently high pressure, i.e., contraction of the interatomic distances, a broadening of the bands will result in the dominance of kinetic energy, which leads to closure of the insulating gap and delocalization

of the  $3d$  electrons [1,5]. Such a transition is commonly referred to as an insulator-to-metal transition (IMT) or a Mott transition. The same mechanism of band broadening has been suggested to be responsible for the pressure induced magnetic collapse in Mott insulators [6]. Indeed, a simultaneous IMT and magnetic collapse have been reported in many Mott insulators both theoretically [7] and experimentally [8,9], which seems to support the idea of an interconnection between insulating behavior and magnetic ordering in this class of compounds.

Applying pressure is a most convenient way to study the nature of the magnetic state in transition-metal oxides and IMTs, since the balance between Coulomb energy and kinetic energy can be tuned directly. Such investigations are important in order to understand the fundamental role of magnetism in solids and its connection to metal-insulator transitions. This becomes increasingly important for understanding novel effects such as superconductivity, in which the intimate link between Mott transitions and the emergence of superconductivity has repeatedly been reported in the literature [10,11].

Although a metallic high-pressure phase of NiO was predicted by Mott *et al.* [1] decades ago, the pressure at which the IMT would occur is still unknown. Considering other  $3d$  metal monoxides, the loss of magnetism occurs above 70 GPa [6,8] in FeO and between 80 and 100 GPa [12,13] in MnO and CoO. In all these cases the magnetic transition is accompanied by a structural transformation. However, NiO in the sodium chloride (B1) structure has so far been found stable up to at least 147 GPa [14].

\*potapkinv@gmail.com

The pressure of the IMT has been studied theoretically, with results ranging between 230 GPa [6] and 3.7 TPa [15]. Due to multiple difficulties in conducting experiments at such ultrahigh pressure, which drastically limits the number of available methods, the amount of experimental work on the actual IMT in NiO is scarce. However, the long-sought IMT in NiO was recently reported to be found at 240 GPa by resistance measurements [16] and authors identified the IMT as a Mott transition.

In all known cases [9], an IMT in Mott insulators has been associated with the loss of magnetic order, and this is expected to apply to NiO as well [6]. Therefore, magnetic investigations are essential to understand the IMT in Mott insulators. However, investigations have so far been hindered by the lack of experimental techniques suitable for probing the antiferromagnetic ordering in NiO under ultrahigh pressure.

The technique commonly used for magnetic studies under pressure, x-ray magnetic circular dichroism, is not suitable in this case, as it cannot be applied to systems which do not have a single ion net magnetization.

Recently, nuclear forward scattering (NFS) was successfully applied to the Mössbauer transition of  $^{61}\text{Ni}$  [17]. Further development of this method has allowed us to investigate the magnetic properties of metallic Ni under the ultrahigh pressure of 260 GPa [18].

In this Rapid Communication, we report an investigation of the magnetic properties of NiO at room temperature up to 280 GPa with  $^{61}\text{Ni}$  NFS (ESRF ID18 [19]), complemented by x-ray diffraction (XRD) (ESRF ID09 [20] and APS 13IDD) and extended x-ray absorption fine structure (EXAFS) (ESRF ID24 [21]) for structural investigations. This is, to the best of our knowledge, the highest pressure at which an EXAFS spectrum has ever been collected. The EXAFS measurements were conducted with the same sample in the same DAC and at the same pressure just after taken the  $^{61}\text{Ni}$  NFS data.

Details about the experimental techniques are provided in the Supplemental Material [22].

The time evolution of the NFS signal, measured at room temperature and at different pressures, is shown in Fig. 1. The measurement at ambient pressure was carried out with a NiO powder (500  $\mu\text{m}$ ) thick. The shape of the spectra in Fig. 1(a) is described by oscillations (quantum beats), due to the magnetic hyperfine splitting of the nuclear levels, that are modulated by the exponential decay with a 7.6 ns lifetime of the excited state in  $^{61}\text{Ni}$  nuclei. Because of the short lifetime most of the spectral weight (the probability to detect a phonon at a given time) is distributed in the first 15 ns of the time spectra. Combined with the decrease of intensity with pressure (thinning of the sample along the beam due to the compression) this results in almost a zero count rate at large times at ultrahigh pressure [Figs. 1(c) and 1(d)]. With the increase of pressure the frequency of the quantum beats increases (the distance between individual beats decreases), while overall the spectrum shrinks but keeps the same shape. The effect is best illustrated by the pressure dependence of the beat that is located furthest from  $t = 0$  in Fig. 1. In Fig. 1(b) this point is located at 37.5 ns, in Fig. 1(c) at 25 ns, and in Fig. 1(d) at 23 ns, further shifting to  $t = 0$ . Taking into account the dependence of the spectral frequency on  $H_{\text{hf}} \times t$ , where  $H_{\text{hf}}$  is the hyperfine magnetic field and  $t$  is the time, the shrinkage is determined by the increasing

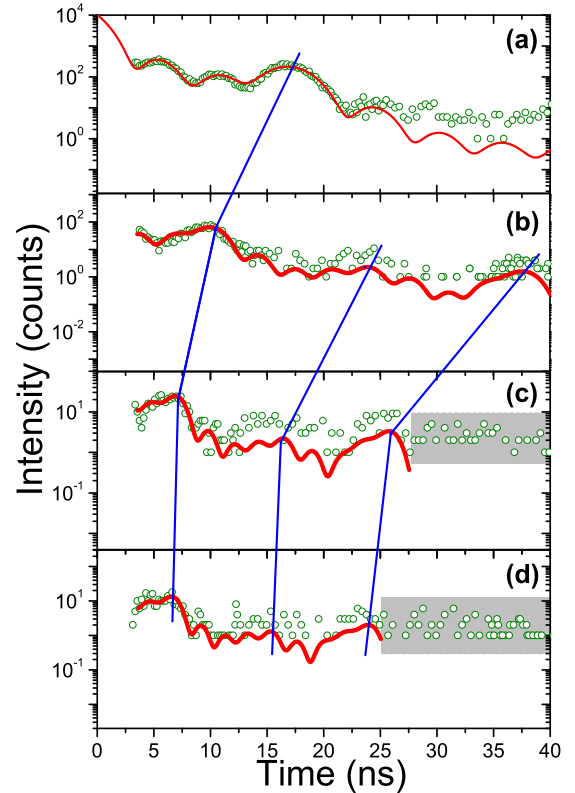


FIG. 1. Time evolution of the nuclear forward scattering for NiO at room temperature at the following pressures: (a) ambient, (b) 39 GPa, (c) 150 GPa, and (d) 280 GPa. The red solid lines show the fit according to the model described in the text. Gray rectangles mark the areas that were not fitted due to insufficient statistics. Blue straight lines are used as a guide for the eyes to track the position shift of the major beats under compression.

magnetic hyperfine field. One can clearly observe the absence of a hyperfine field collapse. If such a collapse would happen, a simple exponential decay of the signal would be observed instead of the present quantum beats. Therefore, the presence of oscillations up to the highest pressure clearly indicates the stability of magnetic order in the system even without fitting the data. The stability of the magnetic order indicates the absence of a Mott type IMT in NiO up to 280 GPa.

Figure 2 shows the measured pressure dependence of the magnetic hyperfine field at room temperature. The magnitude of the hyperfine field at ambient pressure is 8.47(3) T, which is consistent with previous measurements [23]. We find that, upon compression, the magnetic hyperfine field in NiO increases, reaching 24.0(2) T at 280 GPa. The behavior of the hyperfine field in NiO is remarkably different from any known cases, for example, metallic Ni, as seen in Fig. 2. Although the hyperfine field in Ni also initially increases under compression, the increase is only 30%, and above 225 GPa the field starts to decrease [18]. In NiO we observe a steady increase upon compression up to the factor 3.

In order to see if such a behavior could be due to a structural transformation under pressure, we performed XRD and x-ray absorption spectroscopy (XAS) measurements under compression (Fig. 3). The x-ray absorption spectra were

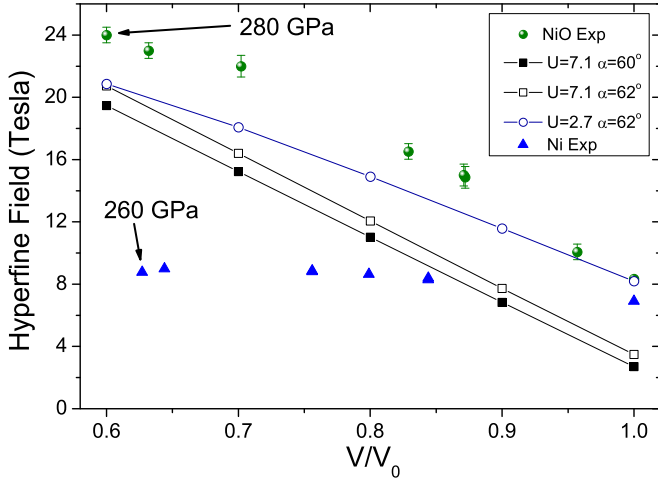


FIG. 2. Pressure dependence of the magnetic hyperfine field in NiO obtained by experiment and *ab initio* calculations within various approximations. Solid olive circles: NiO by NFS; solid black squares: by LSDA +  $U$  for  $U = 7.1$  eV and  $\alpha_R = 60^\circ$ ; open black squares: by LSDA +  $U$  for  $U = 7.1$  eV and  $\alpha = 62^\circ$ ; blue circles: by LSDA +  $U$  for  $U = 2.7$  eV and  $\alpha = 62^\circ$ . Solid blue triangles represent the dependence of the magnetic hyperfine field in Ni by NFS from [18], for comparison. The lines are guides for the eye.

measured up to 280 GPa at the Ni  $K$  edge. Neither in the x-ray absorption near-edge structure, nor in the EXAFS region of the spectra did we observe any changes that could be attributed to any structural and/or electronic phase transitions up to the highest pressure achieved. Thus, all changes we observe in Fig. 3(b) are due to a change in the lattice constants upon compression.

Below  $T_N$ , NiO has a rhombohedral symmetry (space group  $R\bar{3}m$ ), as its ideal cubic B1 structure distorts due to magnetostriction [24,25]. The degree of distortion increases upon cooling [24]. We performed single-crystal diffraction of NiO up to 60(0.5) GPa. Fitting this data with the third-order Birch-Murnaghan equation of state (EOS) (see Fig. 4) results in a bulk modulus of  $K_0 = 170.4(1)$  GPa with the pressure derivative  $K'_0 = 4.35(1)$ .

Powder XRD was measured up to 212(2) GPa [Fig. 3(a)]: the pressure was calculated using the EOS, based on the extracted bulk modulus. We find no indication of any structural transition in the examined pressure region [Fig. 3(a)].

Figure 4 compares the measured volume as a function of applied pressure, obtained by EXAFS and XRD. The resulting EOS agree remarkably well. The very last point is slightly off the curve, most likely due to the well-known effect of compressibility curve deviations at ultrahigh pressure under nonhydrostatic conditions when compared to an EOS obtained at much lower pressure, and under quasihydrostatic conditions.

We have also analyzed the level of rhombohedral distortions under compression. In the top-right inset of Fig. 4, the pressure dependence of the rhombohedral angle  $\alpha$  is plotted. Both the present data and the literature data indicate an increase of  $\alpha$  with pressure. Thus, application of pressure leads to an increasing deviation from cubic symmetry in NiO, as does cooling [24]. The joint XRD/XAS investigation indicates the

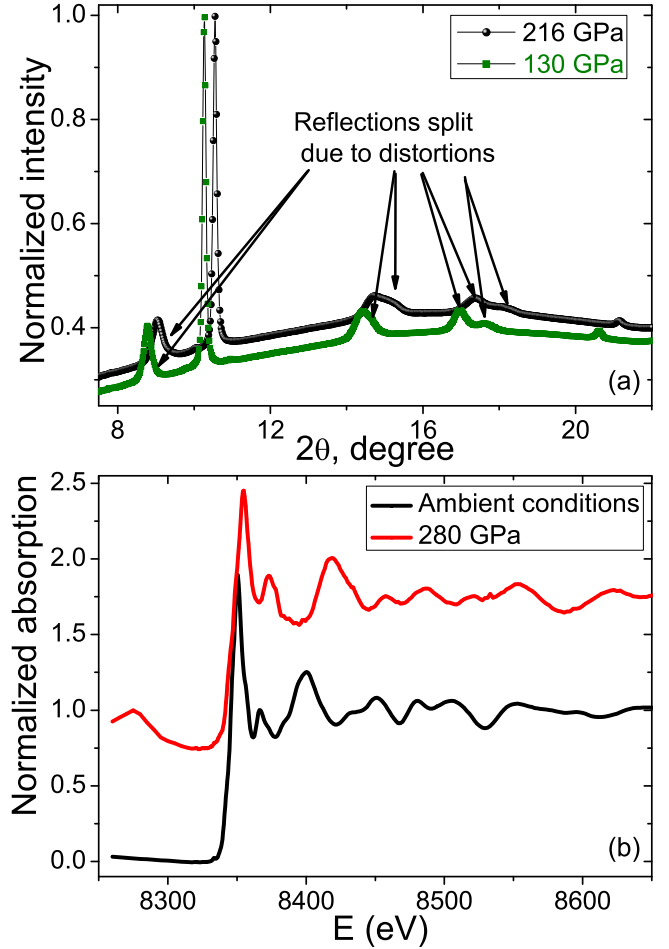


FIG. 3. (a) Diffractograms at 120 and 210 GPa. The arrows show the reflections (111), (202), (213), and (222) that split under pressure due to the rhombohedral distortions. (b) XAS spectra measured at ambient pressure and 280 GPa.

absence of any structural transitions in NiO and the stability of its distorted sodium chloride structure up to 280 GPa. Thus, the threefold increase of the hyperfine field in NiO cannot be explained by any kind of structural transformation.

In order to access the relation between the observed structural and magnetic properties and the insulating gap, we have calculated the hyperfine field of NiO within the framework of density functional theory. We used the local spin density approximation complemented with the Coulomb interaction parameter  $U$  (LSDA +  $U$  method) [22], adopting the value  $U = 7.05$  eV, as calculated in Ref. [26]. Our LSDA +  $U$  calculations reproduce the experimental energy gap at ambient conditions, in agreement with more advanced LSDA + DMFT calculations [26]. This is in contrast to plain local spin-density approximation (LSDA) calculations, which only yield a very narrow gap of 0.4 eV. The XAS spectrum is also well reproduced by our LSDA +  $U$  calculations [22].

In Fig. 2, the calculated hyperfine field is shown along with the experimental data. The pressure evolution of the field is seen to be well reproduced by these calculations (see also Supplemental Material, Fig. 4, in [22]). Taking distortions of

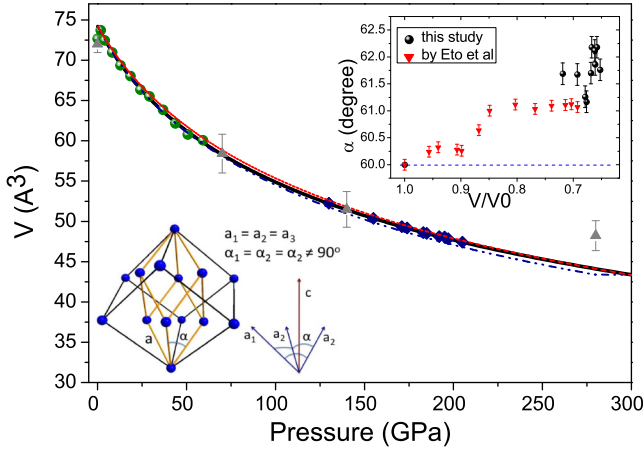


FIG. 4. Pressure dependence of the unit cell volume of NiO. Olive circles: single-crystal XRD measurements; blue diamonds: powder XRD measurements; gray triangles: data calculated from XAS spectra. The black curve is the EOS extracted from single-crystal measurements. For comparison, we have plotted two equations of state found in the literature: dashed red line from [22], and blue dash-dot-dot line from [11]. The top inset shows the volume dependence of the rhombohedral angle  $\alpha$ , as defined in the sketch of the unit cell in the bottom inset. The black dots are values from powder XRD measurements, and red triangles are calculated from [22].

the crystal structure into account (corresponding to  $\alpha = 62^\circ$ ), the field is further increased, improving the agreement with experiment. Note that these results are not very sensitive to the particular choice of  $U$ . Indeed, even with a much smaller value of  $U$ , such as 2.7 eV, the hyperfine field increases in the entire pressure range considered. Most importantly, the magnetic moment remains finite at this pressure, and the band gap remains intact [2]. We therefore conclude that the system has not undergone any IMT.

In order to analyze the mechanism behind the increasing field, we resolve the total hyperfine field into components as follows:

$$H_{\text{hf}} = H_C + H_L + H_{\text{dip}}, \quad (1)$$

where  $H_C$  is the Fermi contact term, i.e., due to the spin density at the nucleus;  $H_L$  is the orbital magnetic field due to the orbital magnetic moment of the electrons; and  $H_{\text{dip}}$  is due to dipole interaction between the nuclear and spin dipole magnetic moments.  $H_{\text{dip}}$  is negligible in the ideal structure, but increases by 1 T when the distortion is applied.

The most significant components in Eq. (1) are  $H_C$  and  $H_L$ , which are oppositely directed.  $H_C$  is larger in magnitude, and is steadily increasing with compression, while  $H_L$  is decreasing [22] along with the orbital magnetic moment. The spin density at the nucleus responsible for  $H_C$  is mainly due to  $s$  electrons locally polarized by the exchange interaction with the  $3d$  electrons. In particular, the main contribution comes from the core electrons of the first and second shells, which are polarized in opposite directions to the valence electrons. These two mutually opposite contributions both decrease upon

compression. However, the valence contribution decreases faster, so that their sum increases.

From the LSDA calculations, corresponding to  $U = 0$ , we note that as the gap closes, there is a dramatic drop in the hyperfine field, which is reduced to the ambient pressure value. This is shown in greater detail in Figs. 4s and 8s of the Supplemental Material [22]. Note that the magnetic moment is finite well into the metallic state. Thus, a finite magnetic moment is not necessarily a direct sign of an insulating state. However, in our measurements, we see no reduction of the hyperfine field. This suggests that no IMT has occurred even at  $V = 0.6V_0$  (300 GPa).

In summary, measurements of the magnetic hyperfine splitting of the Mössbauer spectra show that the antiferromagnetic order in NiO is preserved up to at least 280 GPa. Moreover, the hyperfine field is seen to be increasing in the entire pressure range examined. This observation is well reproduced by our *ab initio* calculations, which also yield a Mott insulator gap in the entire pressure interval of this study. Our results thus indicate the absence of a Mott transition in NiO up to 3 Mbar. This result strongly indicates a direct connection between the stability of antiferromagnetic order and the degree of deviation from perfect cubic symmetry.

The European Synchrotron Radiation Facility is acknowledged for provision of synchrotron radiation beam time and the beamlines ID18 and ID09. The authors thank A. Chumakov and M. Hanfland for their help with ID18 and ID09 experiments, respectively. Portions of this work were performed at GeoSoilEnviroCARS (Sector 13), Advanced Photon Source (APS), Argonne National Laboratory. GeoSoilEnviroCARS is supported by the National Science Foundation–Earth Sciences (Grant No. EAR-1128799) and Department of Energy–GeoSciences (Grant No. DE-FG02-94ER14466). This research used resources of the Advanced Photon Source, a U.S. Department of Energy (DOE) Office of Science User Facility operated for the DOE Office of Science by Argonne National Laboratory under Contract No. DE-AC02-06CH11357. V.Pt. would like to acknowledge Helmholtz Association for support in the framework of the Helmholtz Postdoctoral Program. R.P.H. acknowledges support from the Materials Sciences and Engineering Division, Office of Basic Energy Sciences, U.S. Department of Energy. M.E., J.J., W.O., and I.A.A. acknowledge support from the Swedish Government Strategic Research Area Grants Swedish e-Science Research Center (SeRC) and in Materials Science on Functional Materials at Linköping University (Faculty Grant SFO-Mat-LiU No 2009 00971), as well as from Knut and Alice Wallenbergs Foundation project Strong Field Physics and New States of Matter 2014–2019 (COTXS). I.A.A. is grateful for the support provided by the Swedish Foundation for Strategic Research program SRL Grant No. 10-0026: the Swedish Research Council (VR) Grant No 2015-04391, the Grant of Ministry of Education and Science of the Russian Federation (Grant No. 14.Y26.31.0005), and Tomsk State University Academic D. I. Mendeleev Fund Program. The simulations were carried out using supercomputer resources provided by the Swedish National Infrastructure for Computing (SNIC).



- [1] N. F. Mott, *Metal-Insulator Transitions*, 2nd ed. (Taylor & Francis, London, 1990).
- [2] J. Zaanen, G. A. Sawatzky, and J. W. Allen, *Phys. Rev. Lett.* **55**, 418 (1985).
- [3] N. Hiraoka, H. Okamura, H. Ishii, I. Jarrige, K. D. Tsuei, and Y. Q. Cai, *Eur. Phys. J. B* **70**, 157 (2009).
- [4] G. A. Sawatzky and J. W. Allen, *Phys. Rev. Lett.* **53**, 2339 (1984).
- [5] I. G. Austin and N. F. Mott, *Science* **168**, 71 (1970).
- [6] R. E. Cohen, *Science* **275**, 654 (1997).
- [7] J. Kuné, A. V. Lukoyanov, V. I. Anisimov, R. T. Scalettar, and W. E. Pickett, *Nat. Mater.* **7**, 198 (2008).
- [8] M. P. Pasternak, R. D. Taylor, R. Jeanloz, X. Li, J. H. Nguyen, and C. A. McCammon, *Phys. Rev. Lett.* **79**, 5046 (1997).
- [9] G. K. Rozenberg, M. P. Pasternak, W. M. Xu, L. S. Dubrovinsky, and M. Hanfland, *High Press. Res.* **30**, 238 (2010).
- [10] M.-S. Nam, A. Ardavan, S. J. Blundell, and J. A. Schlueter, *Nature (London)* **449**, 584 (2007).
- [11] P. Durand, G. R. Darling, Y. Dubitsky, A. Zaopo, and M. J. Rosseinsky, *Nat. Mater.* **2**, 605 (2003).
- [12] J.-P. Rueff, A. Mattila, J. Badro, G. Vankó, and A. Shukla, *J. Phys.: Condens. Matter* **17**, S717 (2005).
- [13] C. S. Yoo, B. Maddox, J.-H. P. Klepeis, V. Iota, W. Evans, A. McMahan, M. Y. Hu, P. Chow, M. Somayazulu, D. Häusermann, R. T. Scalettar, and W. E. Pickett, *Phys. Rev. Lett.* **94**, 115502 (2005).
- [14] T. Eto, S. Endo, M. Imai, Y. Katayama, and T. Kikegawa, *Phys. Rev. B* **61**, 14984 (2000).
- [15] X.-B. Feng and N. M. Harrison, *Phys. Rev. B* **69**, 035114 (2004).
- [16] A. G. Gavriluk, I. A. Trojan, and V. V. Struzhkin, *Phys. Rev. Lett.* **109**, 086402 (2012).
- [17] I. Sergueev, A. I. Chumakov, T. H. D. Beaume-Dang, R. Rüffer, C. Strohm, and U. van Bürc, *Phys. Rev. Lett.* **99**, 097601 (2007).
- [18] I. Sergueev, L. S. Dubrovinsky, M. Ekholm, O. Y. Vekilova, A. I. Chumakov, M. Zajac, V. B. Potapkin, I. Kantor, S. Bornemann, H. Ebert, S. I. Simak, I. A. Abrikosov, and R. Rüffer, *Phys. Rev. Lett.* **111**, 157601 (2013).
- [19] R. Rüffer and A. I. Chumakov, *Il Nuovo Cimento D* **18**, 375 (1996).
- [20] M. Merlini and M. Hanfland, *High Press. Res.* **33**, 511 (2013).
- [21] S. Pascarelli, O. Mathon, M. Muñoz, T. Mairs, and J. Susini, *J. Synchrotron Rad.* **13**, 351 (2006).
- [22] See Supplemental Material at <http://link.aps.org/supplemental/10.1103/PhysRevB.93.201110> for details of the experiments and calculations, as well as calculation results on electronic and magnetic properties.
- [23] J. C. Love, F. Obenshain, and G. Czjzek, *Phys. Rev. B* **3**, 2827 (1971).
- [24] H. P. Rooksby, *Acta Cryst.* **1**, 226 (1948).
- [25] W. L. Roth, *Phys. Rev.* **110**, 1333 (1958).
- [26] X. Ren, I. Leonov, G. Keller, M. Kollar, I. Nekrasov, and D. Vollhardt, *Phys. Rev. B* **74**, 195114 (2006).